Vol. 24, No. 3(2025) Alim25592
Revista Mexicana de Ingeniería Química

Development and characterization of antimicrobial bilayer biodegradable films from wheat flour and biopolymers for food packaging

Desarrollo y caracterización de películas biodegradables bicapa con actividad antimicrobiana a partir de harina de trigo y biopolímeros para empaques de alimentos

R.E. González-Cuello[1], J.A. Gómez-Salazar[2], R. Ortega-Toro[1‡]
[1]Professor University of Cartagena, Food Engineering Department, Food Packaging and Shelf-Life research group (FP&SL), Cartagena de Indias D.T. y C., 130015, Colombia;
[2]Profesor Departamento de Alimentos, División de Ciencias de la Vida, Universidad de Guanajuato, Campus Irapuato-Salamanca, C.P.36500 Irapuato, Guanajuato, México.
Sent date: May 16, 2025; Accepted: August 30, 2025

Abstract
This study focuses on the development and characterization of biodegradable bilayer films with antimicrobial properties (against *Bacillus cereus*) formed from wheat flour (WF) monolayers assembled with polycaprolactone (PCL) or Mater-Bi (MB). Monolayer films were made by compression molding, and bilayer films were obtained by bonding a wheat flour layer with a PCL or Mater-Bilayer, incorporating potassium sorbate (PS) and citric acid (CA) as antimicrobial agents at the interface. Film properties were evaluated, including color, gloss, thickness, opacity, internal transmittance, moisture content, water solubility, water absorption capacity, water contact angle, water vapor permeability, mechanical properties, and antimicrobial activity. The results showed that the bilayers with PCL and Mater-Bi offer a better barrier and lower solubility than the wheat flour monolayers and, in turn, show moderate stresses and deformations, with higher elastic moduli, especially in the $B_{WF\text{-}CA\text{-}MB}$ bilayer, which has the highest elastic modulus (174.5 MPa). Also, the inclusion of antimicrobial agents and the combination of varied materials significantly influence the properties of the films, highlighting the antimicrobial effectiveness against *Bacillus cereus*. The study concludes the films offer a sustainable alternative to conventional plastics, improving food safety and extending shelf life in food packaging combining sustainability with functionality. However, additional studies using real food matrices are required to confirm their impact on food safety and product shelf-life extension.
Keywords: Biodegradable packaging, Bilayer films, Wheat flour, Polycaprolactone (PCL), Mater Bi, Antimicrobial activity, *Bacillus cereus*.

Resumen
Este estudio se centra en el desarrollo y la caracterización de películas biodegradables bilaminares con propiedades antimicrobianas (contra *Bacillus cereus*), formadas a partir de monoláminas de harina de trigo (WF) ensambladas con Policaprolactona (PCL) o Mater-Bi (MB). Las películas monolaminares se elaboraron mediante moldeo por compresión, y las películas bilaminares se obtuvieron uniendo una capa de harina de trigo con una de PCL o Mater-Bi, incorporando sorbato de potasio (PS) y ácido cítrico (CA) como agentes antimicrobianos en la interfaz. Se evaluaron diversas propiedades de las películas, incluyendo color, brillo, espesor, opacidad, transmitancia interna, contenido de humedad, solubilidad en agua, capacidad de absorción de agua, ángulo de contacto con el agua, permeabilidad al vapor de agua, propiedades mecánicas y actividad antimicrobiana. Los resultados mostraron que las películas bilaminares con PCL y Mater-Bi ofrecen una mejor barrera y menor solubilidad que las monoláminas de harina de trigo, y presentan esfuerzos y deformaciones moderados, con módulos elásticos más altos, especialmente en la película bilaminar $B_{WF\text{-}CA\text{-}MB}$, que presentó el mayor módulo elástico (174.5 MPa). Asimismo, la inclusión de agentes antimicrobianos y la combinación de distintos materiales influyen significativamente en las propiedades de las películas, destacándose la efectividad antimicrobiana frente a *Bacillus cereus*. El estudio concluye que estas películas representan una alternativa sostenible a los plásticos convencionales, mejorando la seguridad alimentaria y prolongando la vida útil de los productos envasados, al combinar sostenibilidad y funcionalidad. Sin embargo, se requieren estudios adicionales utilizando matrices alimentarias reales para confirmar su impacto en la inocuidad y el tiempo de conservación de los alimentos.
Palabras clave: Envases biodegradables, Películas bilaminares, Harina de trigo, Policaprolactona (PCL), Mater-Bi, Actividad antimicrobiana, *Bacillus cereus*.

‡*Corresponding author. E-mail*: rortegap1@unicartagena.edu.co;
https://doi.org/10.24275/rmiq/Alim25592
ISSN:1665-2738, *issn-e*: 2395-8472

1 Introduction

The search for sustainable solutions has encouraged the development of biodegradable materials, especially in packaging. Biodegradable films, capable of decomposing into natural components through biological processes, have attracted considerable attention in recent research (Moshood *et al*., 2022). Wheat flour has emerged as a promising resource due to its availability, low cost, non-toxicity, and properties (Wang *et al*., 2022). Composed of starch (78-82%) and gluten (8-16%) (Hong *et al*., 2021; Guo *et al*., 2020), wheat flour is among the most abundant sources used as thermoplastic materials for food packaging. However, its use faces challenges related to mechanical and barrier properties (Drakos *et al*., 2018; Dong *et al*., 2022).

Bilayer films have been developed combining wheat flour monolayers with monolayers of biodegradable polymers such as poly(ε-caprolactone) (PCL) and Mater-Bi to overcome these limitations. These combinations improve mechanical and barrier properties and allow the incorporation of antimicrobial agents, such as potassium sorbate, which inhibit microbial growth, prolonging the shelf life of packaged products (Alzate *et al*., 2021; Cheng *et al*., 2024). Furthermore, using citric acid as a linking agent improves the compatibility between the layers, favoring interactions and increasing the cohesion and stability of the bilayer structure (Loukri *et al*., 2024). Integrating natural and synthetic components in these films presents an innovative and sustainable solution for the packaging industry (Avila *et al*., 2022).

Furthermore, the environmental benefits of using renewable resources such as wheat flour and biodegradable polymers contribute to reducing the carbon footprint associated with traditional packaging solutions (Singh *et al*., 2021; Stoica *et al*., 2024). This innovative strategy underlines the potential of developing sustainable packaging materials that meet the growing demand for eco-friendly alternatives in the food industry. On the one hand, using wheat flour as a raw material for manufacturing biodegradable films presents multiple benefits. Firstly, wheat flour is an abundant and low-cost by-product derived from the food industry, making it an economically viable option. Its global availability allows for the reduction of dependence on non-renewable resources, contributing to sustainability. (Stoica *et al*., 2024; Suárez-Castillo *et al*., 2024) Furthermore, wheat flour is rich in carbohydrates, mainly starch, which provides valuable functional properties such as forming films and acting as a binding agent in the film matrix (Wang *et al*., 2022; Petaloti *et al*., 2024).

On the other hand, biodegradable polymers such as polycaprolactone (PCL) and Mater-Bi offer significant advantages in terms of sustainability. PCL, for example, is an aliphatic polymer that decomposes quickly under ambient and non-toxic conditions, minimizing its environmental impact (Thakur *et al*., 2021). Mater-Bi, a biodegradable polymer based on renewable raw materials, decomposes efficiently, and has a favorable environmental profile (Aldas *et al*., 2021). Together, these materials improve the mechanical and barrier properties of films and favor the reduction of plastic waste, offering a sustainable alternative in the packaging industry. The combination of these ingredients allows the creation of packaging solutions that are functional and environmentally friendly and contribute to a circular economy where materials are reused and valued throughout their life cycle.

This study aims to develop bilayer films composed of wheat flour-based monolayers assembled with monolayers of PCL or Mater-Bi, with a focus on evaluating their antimicrobial properties against *Bacillus cereus*, which were assessed exclusively against *Bacillus cereus*.

2 Materials and methods

2.1 Materials

The materials used in this research were carefully selected for their specific properties. The wheat flour, with a humidity of 11.9 % and a composition of total carbohydrates 73 %, protein 12 %, fat 1.4 %, and ash 1.7 %, was purchased from local chain stores in Cartagena. Polycaprolactone (PCL) (average~Mn 80000; density 1.145~g/mL~at 25~°C) was obtained from Sigma-Aldrich and Merck in Bogotá, Colombia, and the Mater-Bi (EF05B, density 1.28 g/cm^3 at 23 °C) was purchased from Novamont, Italy. Glycerol, citric acid, potassium sorbate broths, and microbiological agars, crucial for the process, were supplied by PANREAC, also in Bogotá, Colombia.

2.1.1 Preparation of monolayer films

Monolayer films were fabricated from wheat flour, Mater-Bi, and polycaprolactone (PCL) by compression molding method with previous studies (Moreno-Ricardo *et al*., 2024).

To prepare the wheat flour film, a 4:1 ratio of wheat flour and water was taken; glycerol was additionally incorporated as a plasticizing agent in 25 % of the flour. Then, the ingredients were mixed until a homogeneous mass was obtained and left to rest for 24 h. After this, small portions of 13 g were taken to form the film. These portions were placed in a hydraulic press at a temperature of 120 °C and subjected to pressures from 0 to 100 bar for approximately 2 minutes for each pressure.

Table 1. Mass fractions of the formulations studied (M: monolayers; B: bilayers; WF: wheat flour; PCL: polycaprolactone; MB: Mater-Bi; PS: potassium sorbate; CA: citric acid).

Formulations	WF	PCL	MB	PS	CA
M_{WF}	1	0	0	0	0
M_{PCL}	0	1	0	0	0
M_{MB}	0	0	1	0	0
$B_{WF\text{-}PS\text{-}PCL}$	0.813	0.125	0	0.063	0
$B_{WF\text{-}PS\text{-}MB}$	0.813	0	0.125	0.063	0
$B_{WF\text{-}CA\text{-}PCL}$	0.813	0.125	0	0	0.063
$B_{WF\text{-}CA\text{-}MB}$	0.813	0	0.125	0	0.063

Regarding the preparation of the monolayer PCL and Mater-Bi films, 2 g of each material were weighed. These materials were pressed in the hydraulic press at temperatures of 85 °C for the PCL and 150 °C for the Mater-Bi, with pressures from 0 to 100 bar for approximately 1 minute for each pressure used.

2.2 *Preparation of bilayer films*

The films were obtained following methodologies previously established by other studies (Ortega-Toro, *et al*., 2016). To form the bilayer film, a layer of wheat flour film and a layer of PCL and Mater-Bi were joined at 130 °C and 100 bar pressures for 1 minute. Additionally, antimicrobial agents (potassium sorbate and citric acid) were placed directly at the interface during the assembly of the wheat flour and PCL or Mater-Bilayers. All films were conditioned in desiccators with supersaturated sodium bromide solutions (56% RH) until characterization. Table 1 shows the mass fractions of the studied formulations using a full factorial 2×2 design for the bilayer films, along with additional treatments (controls).

2.2.1 *Characterization of the films*

2.2.1.1 Color

The color was measured with a colorimeter that provided CIE Lab* coordinates, hue angle (h), and chroma or saturation (c). The CIE Lab* coordinates indicate the luminosity on the vertical axis and the orientation towards the color's red, green, blue, and yellow on the horizontal axes (Rivera-Leiva *et al*., 2022). Based on this, the color change was determined by comparing the color of the sample with that of a reference sample. In the case of the bilayer films, color measurements were performed on both sides of the films. Based on this, the color change was determined by comparing the color of the sample with that of a reference sample. The color difference in each coordinate (ΔL, Δb, and Δa) was calculated to do this. The total color difference ΔE^* was calculated using equation (1).

$$\Delta E^* = \sqrt{\Delta L^2 + \Delta b^2 + \Delta a^2} \quad (1)$$

2.2.1.2 Glow

The gloss was measured at an angle of incidence of 60° according to the ASTM D523 standard procedure, using a gloss meter with a flat surface (3NH YG268 multi-angle gloss meter, Minolta, Langenhagen, Germany). Nine films were evaluated, and three readings were taken from each sample. The results were expressed in gloss units (GU).

2.2.1.3 Thickness

The thickness was determined by using a digital micrometer (TL268 TOP EU). Seven random measurements were made of the films, and their average value and standard deviation were recorded.

2.2.1.4 Film opacity

A spectrophotometer (BIOBASE BK-UV1900) was used (Mohammed *et al*., 2023). The films were cut into strips (1 × 3 cm) and affixed to the inner wall of the cuvette for measurement. Opacity was determined using Equation (2):

$$Opacity = \frac{Absorbance\ (600nm)}{Thickness\ (mm)} \quad (2)$$

2.2.1.5 Internal transmittance

For internal transmittance analysis, a spectrophotometer and quartz cells were used. 1 x 3 cm films were introduced into the quartz cells and, subsequently, absorbance data in the UV-visible range (200-800 nm) were obtained. This range was chosen as it covers the wavelengths relevant to the study of internal transmittance (Ortega-Toro *et al*., 2016).

2.2.1.6 Moisture content

The 2x2cm films were dried in a natural convection muffle at 60 °C, maintaining continuous heating until reaching a constant weight. The percentage of humidity was determined using equation (3). Mean values were calculated by averaging three repetitions for each formulation.

$$\%\ Moisture = \frac{W_h - W_s}{W_s} \times 100\% \quad (3)$$

The terms are defined as follows: W_h(Weight hydrated): Weight of the film before drying; W_s (Weight solid): Weight of the film after drying.

2.2.1.7 Water solubility

The films were immersed in distilled water at a ratio of 1:10 (Film: Water) for 48 h. The samples were then dried for 24 h in a natural convection oven at 60 °C to remove free water. Subsequently, they were placed in a desiccator with a saturated sodium bromide (NaBr) solution (RH = 58 %, T = 25 °C) for two weeks to remove bound water. Finally, the percentage of solubility of the films was calculated based on their initial and final weights. This procedure was repeated three times for each formulation and the arithmetic mean obtained was reported (Acevedo-Puello *et al*., 2023).

2.2.1.8 Accumulated water loss and gain

The methodology proposed by Collazo-Bigliardi *et al* (2019) was followed with some adjustments. First, the films were cut into 2x2 cm dimensions and placed in a desiccator with lithium bromide, generating a relative humidity of 6.4% at room temperature. The weight of the films was recorded every 24 h until constant weight (72 h), considering it as well as the weight of the dry film. Next, the films were transferred to a desiccator with a saturated solution of potassium sulfate (97.3 % relative humidity) and weighed every 24 h until the weight was almost constant (72 h), said weight being considered as the wet weight. Finally, graphs representing the accumulated loss or gain of the different formulations were constructed. Each value is the accumulated weight loss or gain in each time interval (Equations 4 and 5). This procedure was performed in triplicate for each formulation.

$$Cumulative\ weight\ loss = P_W - P_t \quad (4)$$

$$Cumulative\ weight\ gain = P_D - P_t \quad (5)$$

P_W = Wet weight of the films
P_t = Weight of the films in the time interval
P_D: Dry weight of the films

2.2.1.9 Contact angle in water

The contact angle was determined as follows: a film sample was placed on a horizontal surface with a white background, and subsequently, a drop of water (with dye) or oil was deposited on the surface of the film. The image was captured with a digital camera after 30 seconds, maintaining a constant distance of 20 cm between the water or oil drop and the camera lens. Finally, the captured image was analyzed using Goniotrans software. In the case of bilayer films, measurements were performed independently on each side due to potential differences in composition and surface behavior. This procedure was performed in triplicate for each formulation, and the average value was reported (Acevedo-Puello *et al*., 2023).

2.2.1.10 Water vapor permeability

The determination was conducted using a gravimetric method following the procedure established in ASTM E96-95, with some modifications. Specific parameters were adjusted to create a humidity gradient from 53 % RH to 100 % at 25 °C. Films without physical defects were selected for water vapor permeability (WVP) testing. Payne permeation cups containing distilled water were used, exposing one side of the film to 100 % RH. These cups and the films were placed in humidity-controlled cabinets at 25 °C, with the relative humidity of the cabinet (53 %) being maintained by supersaturated sodium bromide solutions.

Furthermore, to facilitate the practical use of the films in products with high water activity, the free surface of the film during its elaboration was exposed to a lower relative humidity. The breakers with the films were weighed periodically using a precision analytical balance (0.0001 g). Once the measurements reached a steady state, the water vapor transmission rate (WVTR) was calculated by analyzing the slope of the regression curve and plotting weight loss versus time. This value was then divided by the area of the film. The entire test was performed three times, and the reported results include the average value and the corresponding standard deviation (Muñoz-Suarez *et al*., 2024).

2.2.1.11 Mechanical properties

The fundamental mechanical properties of the analyzed films, including elastic modulus (EM), tensile strength (TS), and elongation (E), were evaluated under controlled conditions of 50 ± 5% relative humidity and 23 ± 2 °C, in accordance with standardized procedures (ASTM D882). The test was performed using a texture analyzer (TX-700 TEXTURE ANALYZER) equipped with a 500 N load cell, operating at a speed of 50 mm/min. The film samples measured 1 mm × 100 mm, with a clamping.

2.2.1.12 Microstructure

The microstructural analysis of the cross-sections of the films was conducted using a scanning electron microscope (JSM-5910, JEOL Ltd., Tokyo, Japan). The film samples were stored in desiccators containing P_2O_5 for two weeks to ensure the absence of water in the samples. Film pieces measuring 0.5 cm^2, were cryofractured, mounted on copper stubs, gold-coated, and examined using an accelerating voltage of 10 kV. Conversely, optical microscopy was performed to analyses the surface of the films. Samples measuring 2 cm^2 were taken to examine their surface using an optical microscope (ZEISS model 415500-1800-000)

at a magnification of 10×. Prior to analysis, the films were conditioned at a relative humidity of 53% and a temperature of 25 °C for one week (Gómez-Contreras *et al*., 2023).

2.2.1.13 Antimicrobial activity against *Bacillus cereus*

The methodology was implemented to evaluate the antimicrobial activity (Aguirre *et al*., 2013), using the agar disc diffusion technique against *Bacillus cereus*, the only microorganism evaluated in this study. Mueller Hinton agar was used as the culture medium, and the bacterium was inoculated by surface seeding. Subsequently, small portions of the films (incorporated with potassium sorbate) were placed around the Petri dish. The plates were incubated at 37 °C for 48 h. After the incubation period, the antimicrobial activity of each material was evaluated by observing the formation of inhibition zones and measuring their diameters in millimeters.

2.3 Statistical analysis

Data analysis was carried out through an ANOVA analysis of variance. The significant differences ($p<0.05$) were evaluated using the Tukey test between the analyses conducted on the different samples. Statistical analyses were performed with Statgraphics Centurion XVI software (Manugistics Corp., Rockville, MD, USA).

3 Results and discussion

3.1 Characterization of the films

3.1.1 Color

Table 2 shows the gloss measurements at 60°, the color parameters (L*, a*, b*, C, h), and the color change (ΔE) value of the formulations. It is observed that the formulations present significant variations in gloss, color, and color change (ΔE). M_{PCL} (pure PCL) has the highest gloss (14.6), indicating a smooth and shiny surface, while M_{MB} (pure Mater-Bi) shows a low gloss (6.0), suggesting a more matte surface. Blends with wheat flour show notable differences between their layers: in $B_{WF\text{-}PS\text{-}PCL}$ and $B_{WF\text{-}PS\text{-}MB}$, the flour layers have a significantly lower gloss than the PCL or Mater-Bi layers. Regarding luminosity (L*), it varies significantly between the formulations, being higher in the pure formulations of M_{PCL} (88.1) and M_{MB} (85.2), which indicates transparent and reflective surfaces. In bilayers that include wheat flour, the lightness is lower, especially in the flour layers, suggesting a darkening effect due to the flour (L* between 76.6 and 79.8). The PCL and Mater-Bi layers in these films maintain a high luminosity, showing that they are brighter than the flour layers. In previous studies, a luminosity close to 90 was reported for M_{PCL} (Gürler *et al*., 2023) and 89 for M_{MB} (Aldas *et al*., 2021), which is consistent with the results obtained in this analysis.

Table 2. Mean values ± standard deviation (SD) is reported of the brightness (GU) and color parameters (luminosity (L*), red/green (a*), yellow/blue (b*), chromaticity (C), and hue angle (h, °) of the films studied. The layer in which the determination is made is indicated in parentheses.

Formulation	Brightness at 60°	Color parameters					ΔE
		L*	a*	b*	C	h	
M_{WF}	14.1±0.7^{ab}	31.1±0.3^{e}	-5.1±0.1^{h}	3.3±0.1^{e}	6.3±0.4^{e}	158.8±0.6^{a}	-
M_{PCL}	14.6±0.8^{a}	88.1±0.3^{a}	-0.3±0.01^{f}	0.6±0.02^{f}	0.9±0.01^{f}	109.2±0.5^{b}	-
M_{MB}	6.0±0.8^{cd}	85.2±0.8^{b}	3.2±0.3^{b}	15.9±0.5^{c}	16.4±0.8^{c}	78.8±0.7^{c}	-
$B_{WF\text{-}PS\text{-}PCL}$ (WF Layer)	5.1±0.4^{d}	77.2±0.6^{d}	-0.9±0.01^{g}	12.7±0.3^{d}	12.8±0.2^{d}	94.1±0.1^{d}	47.3±0.8^{d}
$B_{WF\text{-}PS\text{-}PCL}$ (PCL layer)	13.1±0.4^{b}	77.6±0.4^{d}	-0.9±0.06^{g}	13.2±0.7^{d}	13.1±0.6^{d}	94.0±0.3^{c}	16.41±0.9^{e}
$B_{WF\text{-}PS\text{-}MB}$ (WF layer)	3.8±0.7^{e}	76.6±0.1^{d}	4.8±0.2^{a}	24.7±0.06^{a}	25.2±0.04^{a}	78.8±0.5^{d}	51.4±0.4^{b}
$B_{WF\text{-}PS\text{-}MB}$ (MB layer)	12.7±0.8^{b}	83.6±0.4^{b}	0.3±0.04^{e}	13.1±0.1^{d}	13.1±0.2^{d}	91.6±4.0^{c}	4.4±0.4^{f}
$B_{WF\text{-}CA\text{-}PCL}$ (WF layer)	6.5±0.8^{c}	77.9±0.8^{cd}	-0.5±0.2^{f}	13.1±0.1^{d}	13.4±0.2^{d}	91.6±4.0^{c}	16.1±0.5^{e}
$B_{WF\text{-}CA\text{-}PCL}$ (PCL layer)	14.1±0.7^{ab}	78.8±0.9^{cd}	-0.4±0.02^{f}	12.5±0.7^{d}	12.5±0.8^{d}	91.5±1.1^{c}	48.8±0.5^{c}
$B_{WF\text{-}CA\text{-}MB}$ (WF layer)	5.5±0.8^{cd}	79.8±1.2^{c}	2.4±0.4^{c}	20.8±1.1^{b}	21.1±1.1^{b}	80.73±1.0^{d}	55.4±0.5^{a}
$B_{WF\text{-}CA\text{-}MB}$ (MB layer)	13.7±0.5^{ab}	83.0±1.2^{b}	1.5±0.06^{d}	12.8±0.5^{d}	12.9±0.5^{d}	82.1±1.9^{d}	4.3±0.4^{f}

Different superscript letters in the columns indicate significant differences between the formulations ($p < 0.05$).

Table 3. Mean values ± standard deviation (SD) is reported for thickness (μm), water vapor permeability (WVP, g·mm/kPa·h·m^2), solubility (Sw, g solubilized film/g initial film), moisture content (Xw, g of water/g dry film), and water absorption capacity (Abw, g of dry film/g wet film) of the films studied.

Formulation	Thickness (μm)	WVP	Sw	Abw	Xw
M_{WF}	248.3±0.02^{f}	1.7±0.08^{a}	0.9±0.02^{a}	0.30±0.02^{a}	0.147±0.031^{a}
M_{PCL}	377.7±0.03^{d}	0.3±0.06^{e}	0.008±0.002^{f}	0.11±0.02^{c}	0.034±0.005^{d}
M_{MB}	308.0±0.03^{e}	0.7±0.02^{d}	0.07±0.051^{e}	0.07±0.04^{c}	0.051±0.010^{c}
$B_{WF\text{-}PS\text{-}PCL}$	526.6±0.03^{b}	1.1±0.04^{c}	0.52±0.02^{b}	0.19±0.05^{b}	0.087±0.015^{b}
$B_{WF\text{-}PS\text{-}MB}$	598.0±0.03^{a}	1.3±0.04^{b}	0.84±0.05^{a}	0.20±0.02^{b}	0.081±0.012^{b}
$B_{WF\text{-}CA\text{-}PCL}$	395.3±0.02^{c}	1.1±0.08^{c}	0.15±0.02^{d}	0.18±0.04^{b}	0.071±0.013^{bc}
$B_{WF\text{-}CA\text{-}MB}$	379.9±0.03^{d}	0.8±0.02^{d}	0.36±0.03^{c}	0.20±0.04^{b}	0.065±0.014^{bc}

Different superscript letters in the columns indicate significant differences between the formulations ($p < 0.05$).

Color parameters also varied, with M_{WF} showing greener, less saturated tones, while those with Mater-Bi tended to have more yellow, saturated tones. Differences in color change (ΔE) suggest significant variations in color consistency between formulations. The monolayers (M) showed more uniform gloss and color characteristics defined by the single material. At the same time, the bilayers had more significant variability in gloss and luminosity but with notable chromatic uniformity in the Mater-Bi layers., evidenced by color change (ΔE) values less than 5, which implies that color variations in these layers are insignificant and difficult to detect visually.

3.1.2 Barrier properties

The studied formulations exhibited significant differences in thickness, water vapor permeability (WVP), solubility (Sw), moisture content (Xw), and water absorption capacity (Abw), as shown in Table 3. These variations reflect important distinctions in the physical and functional properties of the films, which are critical for assessing their suitability in packaging applications. The M_{WF} formulation (monolayers composed exclusively of wheat flour) displayed the lowest thickness but showed limited performance, exhibiting the highest values of WVP and solubility. These results suggest that M_{WF} films allow moisture to pass through rapidly, potentially compromising the protection of moisture-sensitive products. Reported WVP values for wheat flour-based films typically range from 1.6 to 2 g/m^2·day, in agreement with the findings of this study (Wang et al., 2022). In contrast, the M_{PCL} formulation showed lower water vapor permeability, indicating superior barrier performance. This improvement is attributed to the hydrophobic nature of poly(ε-caprolactone) (PCL), which reduces both moisture transmission and film solubility, thereby enhancing the protection of packaged food. Meanwhile, the $B_{WF\text{-}PS\text{-}MB}$ formulation, noted for its greater thickness, presented intermediate WVP values but high solubility. This suggests that, although it functions as a moderate moisture barrier, its elevated solubility may compromise structural integrity during prolonged storage. Overall, the bilayer films incorporating PCL and Mater-Bi demonstrated superior barrier properties and lower solubility compared to wheat flour monolayers. This enhanced performance results from the complementary characteristics of the polymers: Mater-Bi, a biodegradable polymer, contributes to mechanical strength and reduced permeability, while PCL improves flexibility and mitigates solubility issues. Collectively, the results highlight the potential of these bilayer formulations to provide effective moisture control while maintaining the structural integrity necessary to extend the shelf life of packaged food products.

3.1.3 Accumulated weight loss and gain from the films

Figure 1 illustrates the accumulated water weight loss of the film formulations over time, providing insight into their dehydration behaviour. As anticipated, the hydrophilic formulations exhibited the highest weight loss due to greater initial hydration levels. Notably, the M_{WF} monolayers showed prominent water loss. In contrast, the M_{PCL} and M_{MB} monolayers retained moisture more effectively, as these materials display lower water affinity. The bilayer films demonstrated intermediate weight loss overall. Among the bilayers, those incorporating monolayers of Mater-Bi lost more moisture compared to those with PCL monolayers, which is consistent with Mater-Bi's greater water affinity than PCL. The addition of citric acid and potassium sorbate at the interface did not significantly influence this property.

In the wheat flour-containing formulations, the hydrophilic nature of starch and gluten likely facilitates water absorption, potentially explaining the observed weight loss, especially in the early stages of the experiment. Additionally, the gradual release of antimicrobial agents such as potassium sorbate and citric acid from the film interfaces could contribute to weight reduction. These water-soluble compounds may migrate to the surface and evaporate or leach under humid conditions (Xu & Li, 2023).

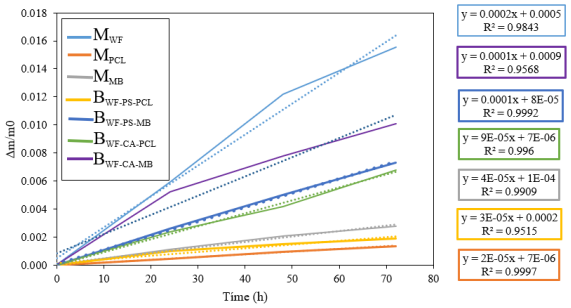

Figure 1. Cumulative weight loss of the films studied, stored at room temperature (25 °C).

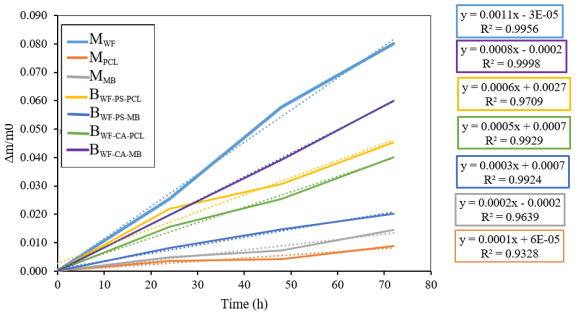

Figure 2. The cumulative weight gain of the films studied was stored at room temperature (25 °C).

Figure 2 shows the accumulated weight gain due to water absorption in the different film formulations. The monolayer made from wheat flour exhibited the highest moisture uptake, a behavior consistent with the hydrophilic nature of starch and gluten present in its composition. In contrast, the PCL monolayer showed the lowest water absorption, followed by the Mater-Bi monolayers. The bilayer films displayed intermediate values between the tested monolayers, highlighting the complementarity of the layers that compose them. This design strategy aims to combine contrasting properties: a hydrophilic layer (wheat flour) and another with lower water affinity (PCL or Mater-Bi). This distinctive feature imparts a balanced moisture response to the developed films, potentially expanding their range of applications in food packaging.

On the other hand, the coefficients of determination (R^2) of both graphs were significantly high, indicating an excellent fit of the data to the proposed linear models. A high R^2 value suggests that a considerable proportion of the variability in the data is explained by the model, implying that the selected independent variables have a significant impact on the dependent variable (Carmona-Cantillo *et al.,* 2025).

3.1.4 Internal transmittance and opacity

Figure 3 shows the UV-Vis transmittance spectra for the monolayers and bilayers studied. Significant variations in transmittance are observed between the different formulations, indicating differences in light absorption, probably due to the chemical composition

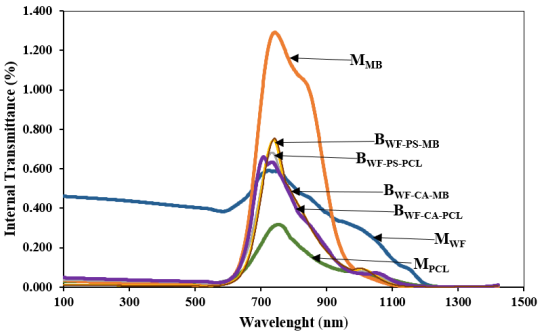

Figure 3. UV-Vis internal transmittance spectra of the different treatments.

and internal structure of the materials. M_{MB} shows a more remarkable ability to allow light to pass through, which could be desirable for applications where transparency is required, while M_{PCL} is the opaquest compared to the others. Furthermore, the other formulations have intermediate UV-Vis transmittance values. This suggests that combinations of wheat flour with additives such as sorbate and citric acid, together with biopolymers (PCL or Mater-Bi), result in materials with optical properties that fall between the high opacity of M_{PCL} and high transparency from M_{MB}. These intermediate values indicate a balance in light transmission, which can be helpful for applications requiring a moderate level of transparency or light protection. This is especially important as continuous exposure to light, particularly ultraviolet light, can compromise food quality as ultraviolet light triggers photolysis and photooxidation reactions, which generate reactive oxygen and free radicals. These compounds result in unpleasant odors and flavors, reduced nutritional value, discoloration, and generally accelerated food degradation (Ezati *et al*., 2023; Nurfani *et al*., 2021).

The opacity data presented in Figure 4 complement the UV-Vis transmittance results discussed previously. The M_{MB} formulation, which exhibited the highest transmittance peak in Figure 3, also shows the highest opacity value (6.4) in Figure 4. This apparent contradiction may be attributed to internal light scattering within the film matrix rather than surface absorption. Conversely, the M_{PCL} formulation, which showed the lowest transmittance peak, also presents a high opacity value (5.5), confirming its opaquer nature. These findings suggest that both materials limit light transmission, although likely through different optical mechanisms.

The optical properties of the films, including color and brightness (Table 1), as well as opacity (Figure 4), are complemented by representative images that allow for the correlation between numerical data and visual appearance. The M_{WF} formulation, composed exclusively of wheat flour, exhibited the lowest brightness value (14.1 ± 0.7) and a reduced L* parameter (31.1 ± 0.3), indicating a darker, matte, and

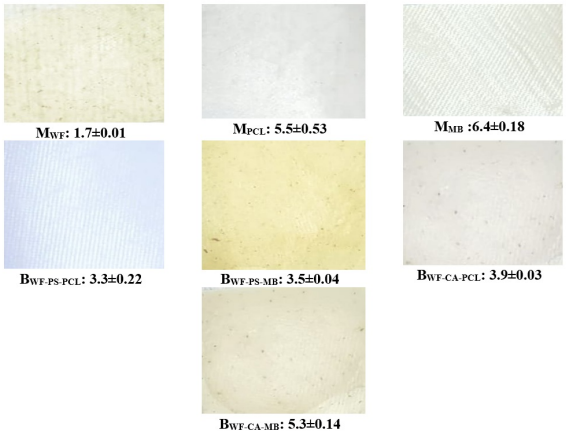

Figure 4. Film appearances from photographs and mean values and standard deviation of the opacity of the monolayer and bilayer films studied. In the bilayers, the PCL or Mater-Bi layer is observed respectively.

less uniform surface. It also showed the lowest opacity (1.7), corresponding to a clearer and more translucent appearance. In contrast, the monolayer films made of PCL and Mater-Bi (M_{PCL} and M_{MB}) displayed higher opacity values (5.5 and 6.4, respectively), along with increased lightness (L* values between 77 and 83), resulting in brighter, more reflective, and less transparent surfaces. The bilayer formulations exhibited intermediate values in both opacity and color, modulated by the combination of biopolymers and additives. Films containing citric acid ($B_{WF\text{-}CA\text{-}MB}$: 5.3 and $B_{WF\text{-}CA\text{-}PCL}$: 3.9) were opaquer than those containing potassium sorbate ($B_{WF\text{-}PS\text{-}PCL}$: 3.3 and $B_{WF\text{-}PS\text{-}MB}$: 3.5). These results demonstrate that the incorporation of wheat flour, PCL, Mater-Bi, and additives allows for the adjustment of the films' optical properties an essential feature for designing packaging materials with varying levels of transparency or light protection, depending on the specific requirements of the product (Drakos *et al*., 2018).

3.1.5 Contact angle

Table 4 shows the values of the contact angle with water and oil indicating the hydrophobicity (CAw) and lipophobicity (CAo) of the films, respectively. Hydrophobicity refers to the ability of a surface to repel water, while lipophobicity is the ability to repel oils. The results showed values less than 90°, which indicates that the films are hydrophilic (CAw) or oleophilic (CAo). This ability to attract water is due to the hydrophilic nature of the starch in wheat flour, which contains hydroxyl groups. These groups form hydrogen bonds with water, making the surface more prone to wetting (Ribero-Sanches *et al*., 2021; Wei *et al*., 2016). These results demonstrate that the contact angle is affected by surface roughness, inhomogeneity, and particle shape and size, where the contact angle values of hydrophilic materials generally decrease with

Table 4. Mean values ± standard deviation (SD) is reported of the contact angle in water (CAw, °) and contact angle in oil (CAo, °) of the monolayer and bilayer films (both sides) studied. The layer in which the determination is made is indicated in parentheses.

Formulations	CAw	CAo
M_{WF}	58.6±1.5^{c}	32.3±2.5^{a}
M_{PCL}	63.0±1.7^{b}	10.3±0.5^{f}
M_{MB}	69.3±2.3^{a}	14.3±1.1^{e}
$B_{WF\text{-}PS\text{-}PCL}$ (WF Layer)	43.3±1.5^{f}	32.2±2.08^{a}
$B_{WF\text{-}PS\text{-}PCL}$ (PCL layer)	58.7±1.5^{c}	16.0±1.0^{de}
$B_{WF\text{-}PS\text{-}MB}$ (WF layer)	52.3±2.1^{de}	22.7±0.6^{c}
$B_{WF\text{-}PS\text{-}MB}$ (MB layer)	67.3±2.0^{ab}	14.7±0.6^{e}
$B_{WF\text{-}CA\text{-}PCL}$ (WF layer)	49.7±2.3^{e}	27.3±0.5^{b}
$B_{WF\text{-}CA\text{-}PCL}$ (PCL layer)	58.6±1.5^{c}	10.6±1.5^{f}
$B_{WF\text{-}CA\text{-}MB}$ (WF layer)	55.3±1.1^{d}	29.6±1.5^{a}
$B_{WF\text{-}CA\text{-}MB}$ (MB layer)	64.7±1.5^{b}	17.3±1.3^{d}

Different superscript letters in columns indicate significant differences between formulations ($p < 0.05$).

increasing roughness of the surface (Gu *et al*., 2016; Balan *et al*., 2021).

The films show more significant variability regarding lipophobicity since M_{PCL} films and bilayers with PCL layers have the lowest contact angles, indicating greater lipophilicity. At the same time, formulations with wheat flour and additives (such as $B_{WF\text{-}CA\text{-}PCL}$ and $B_{WF\text{-}CA\text{-}MB}$) present higher oil contact angles, indicating more oil resistance. These differences show that the composition and structure of the films influence their interaction with liquids, which is crucial in determining their use in specific applications requiring water or oil resistance.

3.1.6 Mechanical properties

The values of the mechanical properties are shown in Table 5 and Figure 5. In general, significant variations are observed in terms of stress (TS), strain (E), and elastic modulus (EM). M_{MB} presents the highest stress (32 MPa) and an intermediate strain (350%), indicating a solid but flexible film. M_{PCL} has the highest strain (1067%), suggesting high elasticity but with lower stress than M_{MB}.

Table 5. Mean values ± standard deviation (SD) is reported for the mechanical parameters: elongation at break (E, %), tensile strength (TS, MPa), and elastic modulus (EM, MPa) of the films studied.

Formulations	TS (Mpa)	E (%)	EM (Mpa)
M_{WF}	7.6 ± 0.2^{d}	140 ± 2^{c}	27.2 ± 1.6^{f}
M_{PCL}	22 ± 2^{b}	1067 ± 22^{a}	314 ± 5^{a}
M_{MB}	32 ± 3^{a}	350 ± 5^{b}	275 ± 3^{b}
$B_{WF-PS-PCL}$	7.5 ± 0.5^{d}	90 ± 2^{d}	114.5 ± 1.5^{e}
$B_{WF-PS-MB}$	6.2 ± 0.2^{e}	140 ± 5^{c}	153.5 ± 1.4^{d}
$B_{WF-CA-PCL}$	11.1 ± 0.3^{c}	120 ± 2^{c}	106.1 ± 0.4^{e}
$B_{WF-CA-MB}$	11.5 ± 0.2^{c}	140 ± 2^{c}	174.5 ± 0.71^{c}

Different superscript letters in columns indicate significant differences between formulations ($p < 0.05$).

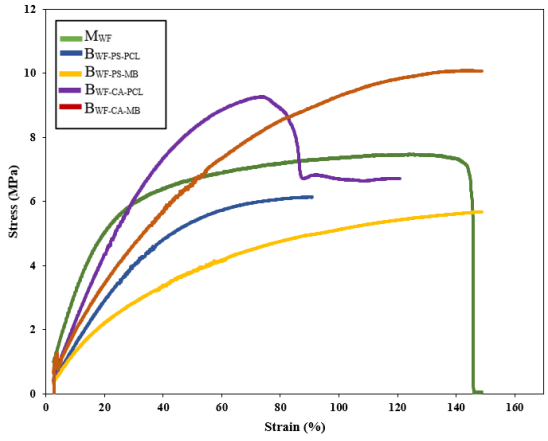

Figure 5. Stress (σ) - deformation (ε) curves of the films studied.

Regarding the bilayers, the bilayer formulations (B_{WF}) with PCL and Mater-Bi show moderate stress and deformations, with higher elastic modulus, especially in $B_{WF\text{-}CA\text{-}MB}$, which has the highest elastic modulus (174.5 MPa), indicating greater rigidity. This suggests that $B_{WF\text{-}CA\text{-}MB}$ could be suitable for applications where a rigid film is required. On the other hand, M_{WF}, with its low values in all parameters, suggests a more brittle and less flexible film, which may not be suitable for certain packaging needs.

As was expected, the WF monolayers exhibited inferior mechanical properties compared to PCL or Mater-Bi. However, when assembled into bilayers, the elastic modulus was significantly improved in all cases, along with tensile strength in those containing citric acid, though deformation capacity remained with no remarkable improvement. These findings are significant, as they illustrate how material properties can be enhanced through a straightforward methodology. The addition of citric acid at the interface appears to further improve these parameters, potentially due to a cross-linking effect exerted by this compound (Sapuła *et al.*, 2023).

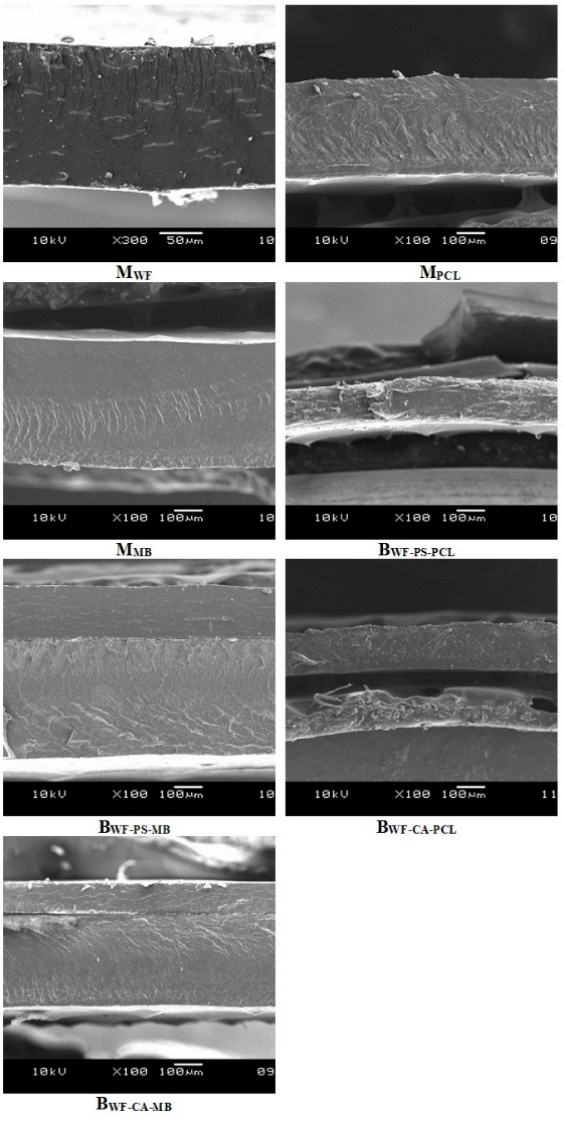

Figure 6. Cross-section SEM micrographs of the studied films.

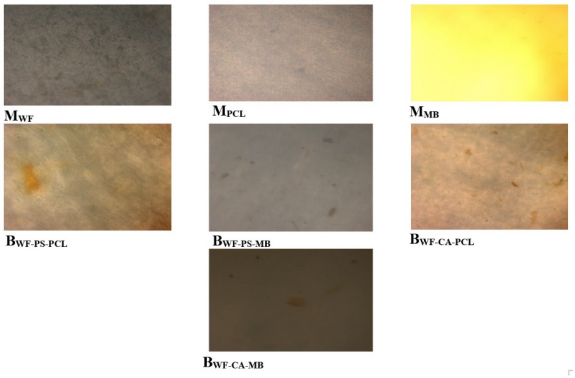

Figure 7. Surface optical micrographs (10X) of the biodegradable films studied. In the bilayers, the PCL or Mater-Bi layer is observed respectively.

3.1.7 Microstructure of the studied films

Figure 6 shows the cross-section of the mono- and bilayers analyzed by SEM. In the monolayers, the cross-sections exhibit some deformations caused by cryofracture. This is particularly evident in the cross-section of M_{PCL}, as polycaprolactone, which has an exceptionally low glass transition temperature (-61.9 °C) (Ortega-Toro *et al*., 2016), demonstrated greater resistance to cryofracture with liquid nitrogen. This same characteristic led to the detachment of bilayers containing PCL during cryofracture, both in the presence of potassium sorbate and citric acid. In contrast, the bilayers containing Mater-Bi exhibited good adhesion, as observed in both $B_{WF\text{-}PS\text{-}MB}$ and $B_{WF\text{-}CA\text{-}MB}$. This is a positive indicator for the development of bilayer materials composed of wheat flour and Mater-Bi, using citric acid and potassium sorbate as interfacial agents, as interfacial adhesion was maintained even under extremely low temperatures and mechanical stress (cryofracture conditions in the SEM technique).

Figure 7 presents optical micrographs taken at 10X magnification showing the surface of the studied biodegradable films. These micrographs allow us to observe the differences in each type of film's texture, structure, and possible surface defects.

Figure 8 presents 2.5D surface optical micrographs at 10× magnification, illustrating the topography and texture of the analyzed biodegradable films. These images reveal significant differences in surface roughness and homogeneity among the various formulations. The monolayer M_{MB} exhibits the smoothest and most homogeneous surface, suggesting high compatibility among its components. In contrast, formulations containing wheat flour, such as M_{WF}, display greater surface roughness, possibly due to the presence of particles of varying sizes, such as non-gelatinized starch, proteins (gluten), and fibers. Regarding bilayer films, $B_{WF\text{-}CA\text{-}MB}$ and $B_{WF\text{-}PS\text{-}PCL}$ demonstrate greater interfacial homogeneity, which may be attributed to the plasticizing and compatibilizing effects of citric acid (CA) and potassium sorbate (PS). These compounds may diffuse into the Mater-Bi and PCL layers during thermal pressing, promoting better integration between layers and reducing interfacial roughness. Such microstructural differences directly influence the films' physical properties, affecting characteristics such as adhesion, permeability, and mechanical performance. This highlights the relevance of surface morphology in the design of biodegradable materials for packaging applications.

M_{MB} presents the smoothest and most homogeneous surface compared to all, while formulations that include wheat flour usually show greater heterogeneity in texture. This finding is significant in the field of materials science as it provides

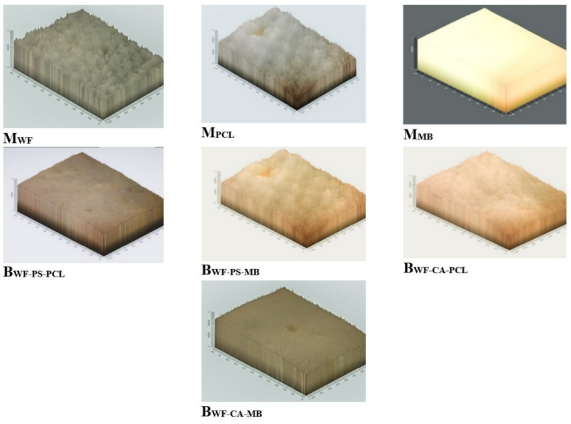

Figure 8. 2.5D (10X) surface optical micrographs of the biodegradable films studied. In the bilayers, the surface of the wheat flour monolayer is observed.

insights into the surface properties of biodegradable films. In addition, M_{WF} presents a roughness that may be related to the presence of particles of varied sizes such as non-gelatinized starch, proteins such as gluten, and fibers (Balan *et al*., 2021).

It is worth mentioning that the $B_{WF\text{-}PS\text{-}PCL}$ and $B_{WF\text{-}CA\text{-}MB}$ combinations presented greater homogeneity between the bilayers; this may be because wheat flour provides heterogeneity due to its granular structure and its combination with citric acid or potassium sorbate. It mitigates this effect since it acts as a plasticizer that helps improve the dispersion and integration of the components. The particles of different sizes may be related to non-gelatinized starch and proteins such as gluten and fibers.

3.1.8 Antimicrobial activity against Bacillus cereus

Figure 9 shows the inhibition zones of bilayer films based on wheat flour and Mater-Bi incorporated with 10% potassium sorbate against *Bacillus cereus*. Specifically, the image corresponds to the $B_{WF\text{-}PS\text{-}MB}$ film, where a clear zone is observed around the sample, indicating the inhibition of Bacillus cereus growth due to the presence of potassium sorbate. This suggests that the compound plays a significant role in microbial inhibition. The inhibition zones observed in this experiment reflect the effectiveness of the films in preventing bacterial growth, measured by the diameter of the areas where microbial proliferation was suppressed. Potassium sorbate is a preservative with antimicrobial properties (Kowalczyk *et al*., 2020), primarily used to inhibit the growth of bacteria, fungi, and yeasts (Marínez-Tenorio *et al*., 2024; Martins *et al*., 2022). Similar studies have demonstrated that incorporating 10% and 2.5% potassium sorbate into wheat gluten films plasticized with glycerol can inhibit the growth of *Aspergillus niger* and *Fusarium incarnatum*, respectively. In that study, the wheat gluten films released a significant amount of potassium sorbate when in contact with an absorbent medium, such as agar

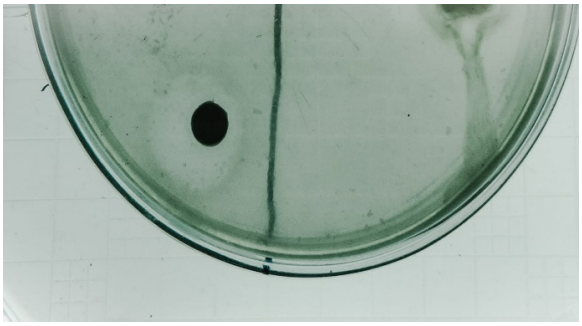

Figure 9. Inhibition zones of bilayer films based on wheat flour and Mater-Bi incorporated with 10% potassium sorbate against the bacteria *Bacillus cereus*.

Table 6. Mean values ± standard deviation (SD) is reported of the inhibition diameters against *Bacillus cereus* of the studied bilayers.

Optimal formulations	Inhibition diameter (mm)
$B_{WF\text{-}PS\text{-}PCL}$	6.0±1.4[a]
$B_{WF\text{-}PS\text{-}MB}$	5.5±0.2[a]

Different superscript letters in the columns indicate significant differences between the formulations ($p < 0.05$).

solution. This indicates that, with further development and optimization, these films could be applied as active edible packaging materials, capable of releasing the antimicrobial agent into food to help prevent the proliferation of microorganisms (Türe *et al*., 2012).

Table 6 presents the inhibition diameter values of the bilayer films studied. The results of the antimicrobial activity against *Bacillus cereus* indicate that the evaluated films exhibited a certain capacity to inhibit the growth of this microorganism, although to a limited extent. In particular, the $B_{WF\text{-}PS\text{-}PCL}$ formulation showed a larger inhibition diameter than $B_{WF\text{-}PS\text{-}MB}$. Therefore, $B_{WF\text{-}PS\text{-}PCL}$ was slightly more effective in stopping the bacteria's growth than $B_{WF\text{-}PS\text{-}MB}$. However, the higher standard deviation for $B_{WF\text{-}PS\text{-}PCL}$ suggests more variability in the measure of the inhibition zone with this formulation. In contrast, the low standard deviation of $B_{WF\text{-}PS\text{-}MB}$ indicates that the results were more uniform and consistent. On the other hand, the observed inhibition zones are relatively small, indicating that the films have a limited capacity to combat *Bacillus cereus* on the red arrow.

Conclusions

In conclusion, the study demonstrates that bilayer films made with PCL and Mater-Bi, combined with wheat flour and antimicrobial agents, present improved properties compared to wheat flour monolayers. These bilayers offer a better water vapor barrier, lower solubility and higher gloss, and more excellent color uniformity, making them more suitable for applications in biodegradable food packaging. The incorporation of PCL and Mater-Bi not only improves the functionality of the films by providing higher opacity and strength but also contributes to their potential as sustainable alternatives in the packaging industry. Therefore, these formulations represent a promising option for combining sustainability and food preservation efficacy. Future applications may include packaging for perishable goods, where enhanced barrier properties and antimicrobial activity can effectively preserve food quality. Overall, this research paves the way for innovative, eco-friendly solutions in food packaging that marry sustainability with functionality.

Funding

This research was funded by Universidad de Cartagena, Strengthening Project Act 048-2023.

Acknowledgements

Special thanks to engineer Diana Paola Carmona for her support in conducting this work.

References

Acevedo-Puello, V., Figueroa-López, K.J. and Ortega-Toro, R. (2023). Gelatin-based hydrogels containing microcrystalline and nanocrystalline cellulose as moisture absorbers for food packaging applications. *Journal of Composites Science 7(8)*, 337. https://doi.org/10.3390/jcs7080337

Aguirre, A., Borneo, R. and León, A.E. (2013). Antimicrobial, mechanical and barrier properties of triticale protein films incorporated with oregano essential oil. *Food Bioscience 1*, 2–9. https://doi.org/10.1016/j.fbio.2012.12.001

Aldas, M., Pavon, C., Ferri, J. M., Arrieta, M. P., and López-Martínez, J. (2021). Films based on Mater-Bi® compatibilized with pine resin derivatives: optical, barrier, and disintegration properties. *Polymers,* 13(9), 1506. https://doi.org/10.3390/polym13091506

Alzate, P., Gerschenson, L., and Flores, S. (2021). Study of the performance of particles based on modified starches containing potassium sorbate and incorporated into biodegradable films: Physicochemical characterization and antimicrobial action. *Chem, 3*(2), 658–671. https://doi.org/10.3390/chemistry3020046

ASTM International. *Standard Test Method for Specular Gloss*. 1999;523–89.

Avila, L.B., Pinto, D., Silva, L.F.O., de Farias, B.S., Moraes, C.C., Da Rosa, G.S. and Dotto, G. (2022). Antimicrobial bilayer film based on chitosan/electrospun zein fiber loaded with jaboticaba peel extract for food packaging applications. *Polymers 14(24)*, 5457. https://doi.org/10.3390/polym14245457

Balan, G.C., Paulo, A.F.S., Correa, L.G., Alvim. I.D., Ueno, C.T., Coelho, A.R., Stroher, G.R., Yamashita, F., Sakanaka, L.S. and Shirai, M.A. (2021). Production of wheat flour/PBAT active films incorporated with oregano oil microparticles and its application in fresh pastry conservation. *Food and Bioprocess Technology 14(8)*, 1587–99. https://doi.org/10.1007/s11947-021-02659-2

Carmona-Cantillo, D., López-Padilla, A., & Ortega-Toro, R. (2025b). Innovation in Biodegradable Composites: Wheat Flour and *Hermetia illucens* Larvae Flour Biocomposites Enhanced with Cellulose Nanocrystals. *Journal of Composites Science* 2025, Vol. 9, Page 249, 9(5), 249. https://doi.org/10.3390/JCS9050249

Cheng, S., Yin, C., Li, K., Liu, Z., Pan, Q., Zuo, X., Guo, A. and Ma, H. (2024). Preparation and characterization of probiotic *Bacillus velezensis* 906 metabolites /potassium sorbate/ polyvinyl alcohol antimicrobial blend film. *Food Bioscience 61*, 104633. https://doi.org/10.1016/j.fbio.2024.104633

Collazo-Bigliardi, S., Ortega-Toro, R. and Chiralt, A. (2019). Improving properties of thermoplastic starch films by incorporating active extracts and cellulose fibres isolated from rice or coffee husk. *Food Packaging and Shelf Life 22*, 100383. https://doi.org/10.1016/j.fpsl.2019.100383

Dong, M., Tian, L., Li, J., Jia, J., Dong, Y., Tu, Y., Liu, X., Tan, C. and Duan, X. (2022). Improving physicochemical properties of edible wheat gluten protein films with proteins, polysaccharides and organic acid. *LWT 154*, 112868. https://doi.org/10.1016/j.lwt.2021.112868

Drakos, A., Pelava, E. and Evageliou, V. (2018). Properties of flour films as affected by the flour's source and particle size. *Food Research International 107*, 551–8. https://doi.org/10.1016/j.foodres.2018.03.005

Ezati, P., Khan, A., Priyadarshi, R., Bhattacharya, T., Tammina, S.K. and Rhim, J.W. (2023) Biopolymer-based UV protection functional films for food packaging. *Food Hydrocolloids 142*, 108771. https://doi.org/10.1016/j.foodhyd.2023.108771

Gómez-Contreras, P., Hernández-Fernández, J. and Ortega-Toro, R. (2023). Obtención y caracterización de colágeno del pez de agua dulce *Prochilodus magdalenae*: aplicación en películas biodegradables. *Información Tecnológica 34(2)*, 89–98. https://doi.org/10.1016/j.ijbiomac.2021.10.075

Gu, H., Wang, C., Gong, S., Mei, Y., Li, H. and Ma, W. (2016) Investigation on contact angle measurement methods and wettability transition of porous surfaces. *Surface and Coatings Technology 292*, 72–7. https://doi.org/10.1016/j.surfcoat.2016.03.014

Guo, L., Fang, F., Zhang, Y., Xu, D., Xu, X. and Jin, Z. (2020). Effect of glutathione on gelatinization and retrogradation of wheat flour and starch. *Journal of Cereal Science 95*, 103061. https://doi.org/10.1016/j.jcs.2020.103061

Gürler, N., Pekdemir, M.E., Torğut, G. and Kök, M. (2023). Binary PCL–waste photopolymer blends for biodegradable food packaging applications. *Journal of Molecular Structure 1279*, 134990. https://doi.org/10.1016/j.molstruc.2023.134990

Hong, J., An, D., Wang, M., Liu, C., Buckow, R., Li, L., Zheng, X. and Bian, K. (2021). Wheat noodles enriched with A-type and/or B-type wheat starch: physical, thermal and textural properties of dough sheet and noodle samples from different noodle-making process. *International Journal of Food Science & Technology 56(6)*, 3111–22. https://doi.org/10.1111/ijfs.14954

Kowalczyk, D., Kordowska-Wiater, M., Karaś, M., Zięba, E., Mężyńska, M. and Wiącek, A.E. (2020). Release kinetics and antimicrobial properties of the potassium sorbate-loaded edible films made from pullulan, gelatin and their blends. *Food Hydrocolloids 101*, 105539. https://doi.org/10.1016/j.foodhyd.2019.105539

Loukri, A., Kyriakoudi, A., Oliinychenko, Y., Stratakos, A.C., Lazaridou, A. and Mourtzinos, I. (2024). Preparation and characterization of chitosan-citric acid edible films loaded with Cornelian cherry pomace extract as active packaging materials. *Food Hydrocolloids 150*, 109687. https://doi.org/10.1016/j.foodhyd.2023.109687

Martínez-Tenorio, Y., Ramírez-Corona, N., Jiménez-Munguía M.T., López-Malo, A. and Mani-López, E. (2024). Development of antifungal packaging from low-density polyethylene with essential oil of oregano and potassium sorbate. *Packaging Technology and Science 37(7)*, 641–53. https://doi.org/10.1002/pts.2813

Martins, M.P., de Sousa, R.S., Dagostin, J.L.A., Franco, T.S; de Muñiz, G.I.B. and Masson, M.L. (2022). Impact of clove essential oil and potassium sorbate incorporation on cassava starch-based films reinforced peach palm cellulose nanofibrils. *Journal of Food Processing and Preservation 46(10)*, e16867. https://doi.org/10.1111/jfpp.16867

Mohammed, A.A.B.A., Hasan, Z, Omran A.A., Elfaghi, A.M., Ali, Y.H., Akeel, N.A.A., Ilyas, R.A. and Sapuan, S.M. (2023). Effect of sugar palm fibers on the properties of blended wheat starch/polyvinyl alcohol (PVA) -based biocomposite films. *Journal of Materials Research and Technology 24*, 1043–55. https://doi.org/10.1016/j.jmrt.2023.02.027

Moreno-Ricardo, M.A., Gómez-Contreras, P., González-Delgado, Á.D., Hernández-Fernández, J. and Ortega-Toro, R. (2024). Development of films based on chitosan, gelatin and collagen extracted from bocachico scales (*Prochilodus magdalenae*). *Heliyon 10(3)*, e25194. https://doi.org/10.1016/j.heliyon.2024.e25194

Moshood, T.D., Nawanir, G., Mahmud, F., Mohamad, F., Ahmad, M.H. and AbdulGhani, A. (2022). Sustainability of biodegradable plastics: new problem or solution to solve the global plastic pollution? *Current Research in Green and Sustainable Chemistry 5*, 100273. https://doi.org/10.1016/j.crgsc.2022.100273

Muñoz-Suarez, A. M., Cortés-Rodríguez, M., & Ortega-Toro, R. (2024). Biodegradable films based on tilapia collagen (Oreochromis sp): improvement of properties with PLA and PCL bilayers with potential use in sustainable food packaging. *Revista Mexicana de Ingeniera Química,* 23(3). https://doi.org/10.24275/rmiq/Alim24326

Nurfani, E., Lailani, A., Kesuma, W.A.P., Anrokhi, M.S., Kadja, G.T.M. and Rozana, M. (2021). UV sensitivity enhancement in Fe-doped ZnO films grown by ultrafast spray pyrolysis. *Optical Materials 112*, 110768. https://doi.org/10.1016/j.optmat.2020.110768

Ortega-Toro, R., Collazo-Bigliardi, S., Talens, P. and Chiralt, A. (2016). Influence of citric acid on the properties and stability of starch-polycaprolactone based films. *Journal of Applied Polymer Science 133(2)*. https://doi.org/10.1002/app.42220

Ortega-Toro, R., Santagata, G., Gomez, G., Cerruti, P., Talens, P., Chiralt, A. and Malinconico, M. (2016). Enhancement of interfacial adhesion between starch and grafted poly(ε-caprolactone). *Carbohydrate Polymers 147*, 16-27. https://doi.org/10.1016/j.carbpol.2016.03.070

Petaloti, A.I., Makri, S., and Achilias, D.S. (2024). Bioactive edible gel films based on wheat flour and glucose for food packaging applications. *Gels 10(2)*, 105. https://doi.org/10.3390/gels10020105

Ribeiro-Sanches, M.A., Camelo-Silva, C., Tussolini, L., Tussolini, M., Zambiazi, R.C. and Becker-Pertuzatti, P. (2021). Development, characterization and optimization of biopolymers films based on starch and flour from jabuticaba (*Myrciaria cauliflora*) peel. *Food Chemistry 343*, 128430. https://doi.org/10.1016/j.foodchem.2020.128430

Rivera Leiva, A.F., Hernández-Fernández, J. and Ortega-Toro, R. (2022). Active films based on starch and wheat gluten (*Triticum vulgare*) for shelf-life extension of carrots. *Polymers 14(23)*, 5077. https://doi.org/10.3390/polym14235077

Sapuła, P., Bialik-Wąs, K., & Malarz, K. (2023). Are Natural Compounds a Promising Alternative to Synthetic Cross-Linking Agents in the Preparation of Hydrogels? *Pharmaceutics 2023, Vol. 15, Page 253*, *15*(1), 253. https://doi.org/10.3390/PHARMACEUTICS1501025

Shen, G., Yu, G., Wu, H., Li, S., Hou, X., Li, M., Li, Q., Liu, X., Zhou, M., Chen, A. and Zhang, Z. (2021). Incorporation of lipids into wheat bran cellulose/wheat gluten composite film improves its water resistance properties. *Membranes*, *12(1)*, 18. https://doi.org/10.3390/membranes12010018

Singh, R., Sharma, R., Shaqib, M., Sarkar, A., and Chauhan, K.D. Biodegradable polymers as packaging materials. (2021). In *Biopolymers and their industrial applications*. Pp. 245-259. Elsevier. https://doi.org/10.1016/B978-0-12-819240-5.00010-9

Stoica, M., Bichescu, C.I., Crețu, C. M., Dragomir, M., Ivan, A.S., Podaru, G.M., ... and Stuparu-Crețu, M. (2024). Review of bio-based biodegradable

Polymers: smart solutions for sustainable food packaging. *Foods 13(19)*, 3027. https://doi.org/10.3390/foods13193027

Suárez-Castillo, G. M., Salcedo-Guadalupe, J. G., Contreras-Lozano, K. P., Rangel-Pérez, M. G., Cervera-Ricardo, M. A., & Figueroa-Flórez, J. A. (2024). Increase in the degree of substitution of cassava starches by dual modification processes. *Revista Mexicana de Ingeniera Quimica*, 23(3). https://doi.org/10.24275/RMIQ/POLY24303

Thakur, M., Majid, I., Hussain, S. and Nanda, V. (2021). Poly (ε-caprolactone): a potential polymer for biodegradable food packaging applications. *Packaging Technology and Science 34(8)*, 449-461. https://doi.org/10.1002/pts.2572

Türe, H., Gällstedt M. and Hedenqvist, M.S. (2012). Antimicrobial compression-moulded wheat gluten films containing potassium sorbate. *Food Research International 45(1)*, 109–15. https://doi.org/10.1016/j.foodres.2011.10.012

Wang, J., Sun, X., Xu, X., Sun, Q., Li, M., Wang, Y. and Xie, F. (2022). Wheat flour-based edible films: effect of gluten on the rheological properties, structure, and film characteristics. *International Journal of Molecular Sciences 23 (19)*, 11668. https://doi.org/10.3390/ijms231911668

Wei, B., Sun, B., Zhang, B., Long, J., Chen, L. and Tian, Y. (2016). Synthesis, characterization and hydrophobicity of silylated starch nanocrystal. *Carbohydrate Polymers 136*, 1203–8. https://doi.org/10.1016/j.carbpol.2015.10.025

Xu, J., & Li, Y. (2023). Wheat glutenbased coatings and films: preparation, properties, and applications. *Journal of Food Science*, *88*(2), 582–594. https://doi.org/10.1111/1750-3841.16454;WGROUP:STRING:PUBLICATION